2022 International Conference on Computational Science and Computational Intelligence (CSCI) | 979-8-3503-2028-2/22/$31.00 ©2022 IEEE | DOI: 10.1109/CSCI58124.2022.00317

Computational Analysis of a Light-Weight SUVr Processing Technique for Neuroimaging Alzheimer's Disease

Robin Perry Mayrand
Electrical & Computer Engineering
Florida International University
Miami FL, USA
rmayr002@fiu.edu

Christian Yaphet Freytes
Electrical & Computer Engineering
Florida International University
Miami FL, USA
cfrey001@fiu.edu

Luana Okino Sawada
School of Computing & Information Sciences
Florida International University
Miami FL, USA
lokin001@fiu.edu

Micheal Adeyosoye
Electrical & Computer Engineering
Florida International University
Miami FL, USA
madey004@fiu.edu

Rosie E. Curiel Cid
Department of Neuropsychology
University of Miami
Miami FL, USA
rcuriel2@med.miami.edu

David Lowenstein
Cognitive Neurosciences and Aging
University of Miami
Miami FL, USA
dloewenstein@med.miami.edu

Ranjan Duara
Wien Center for Alzheimer's Disease and Memory Disorders
Mt Sinai Medical Center
Miami FL, USA
ranjan.duara@msmc.com

Malek Adjouadi
Electrical & Computer Engineering
Florida International University
Miami, United States
adjouadi@fiu.edu

***Abstract*—The Standard Uptake Value (SUV) is conventionally calculated using the ratio of the injected PET radiotracer dose and subject body weight (B_{inj}). SUVs are used to obtain SUV ratios (SUVr), an important metric in many Alzheimer's Disease (AD) neuroimaging studies. However, SUVr can be obtained using only neuroimaging data, bypassing the need for B_{inj}. This paper proposes the SUVr-LightWeight (SUVr-LW) algorithm which is not reliant on clinical data and instead focuses on PET intensity values. The SUVr-LW was evaluated using the Centiloid Project Florebetaben (FBB) subject cohort and reached a linear regression slope of 0.98, while the healthy control subjects produced a slope of 0.87.**

***Index Terms*—Alzheimer's Disease, Neuroimaging, SUVR, Amyloid PET, MRI**

I. Introduction

In diagnosing Alzheimer's Disease (AD), medical experts depend primarily on different methodologies of mental examinations and clinical data [1]. Neuroimaging modalities such as Magnetic Resonance Imaging (MRI) and Positron Emission Tomography (PET), which are integral components for assessing brain structures and functionality, have become essential imaging modalities for the diagnosis and understanding of AD and its related effects on the structure and functionality of the brain [2]. Recent efforts have leveraged the amount of quantitative data that can be extracted from the neuroimaging modality via automatic brain segmentation of an MRI T1-sequenced image of a brain with software tools such as FreeSurfer [3] and the Statistical Parametric Mapping (SPM) toolbox [4] which are capable of automatic segmentation of an MRI image into the brain's individual regions of interest (ROI). PET scans have been uniquely useful in the accurate detection of AD via radiotracers that bind to specific biomarkers such as Beta-Amyloid binding radiotracers, which include F-18 Florbetaben (FBB), F-18 Florbetapir (AV45), and C-10 Pittsburgh compound B (PiB) [5].

As the research and amount of data collected grows, there arises the issue of cross-site comparison. Using image processing techniques, the voxel intensity values of PET modality can be gathered and then normalized by some subject-specific factor B_{inj} to yield a Standardized Uptake Value (SUV) [6]. SUVs can then be normalized across the brain by different composite regions such whole cerebellum, cerebellar grey matter, or a composite region [7] creating an SUV ratio (SUVr). The SUVr is vital in comparing radiotracer binding indexes across PET images generated with the same radiotracer [8]. However, multiple radiotracers are often used for the same purpose due to their different absorption behaviours but the resulting SUVs cannot be compared across tracers. The Centiloid Project [9] devised a set of scaling formulas to calibrate all PET radiotracers for use in cross-cohort studies

This research is supported by the National Science Foundation under grants: CNS-1920182, CNS-2018611, and CNS-1551221, and with the National Institutes of Health through the P30AG066506 with the 1Florida Alzheimer's Disease Research Center (ADRC).

2769-5654/22/$31.00 ©2022 IEEE
DOI 10.1109/CSCI58124.2022.00343

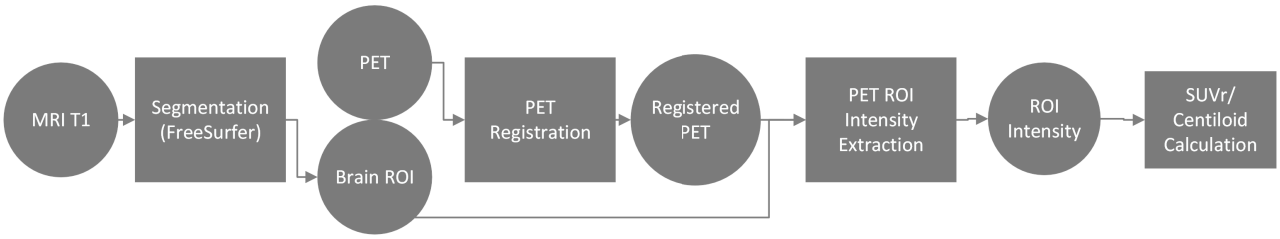

Fig. 1. Flowchart of the proposed pipeline flow: MRI-specific data/files are marked in blue, PET in red, and combined modalities in purple.

through use of the Centiloid Score. This study proposes the use of a PET intensity value K to directly calculate SUVr and the Centiloid Score to demonstrate SUVr-LW.

The rest paper is structured as follows: $Section\ II$ describes the tools and processes used throughout the SUVr-LW, $Section\ III$ compares and statistically evaluates the SUVr-LW against a Centiloid Project calibration dataset, and $Section\ IV$ concludes the paper, discusses the limitations, and offers future direction for the research.

II. Methods

A. Dataset

This study makes use of the Global Alzheimer's Association Interactive Network (GAAIN) Centiloid Project [9] FBB PET calibration dataset aimed at onboarding new study centers into their network. The dataset detailed in Table I consists of 10 young healthy control subjects (aged $\leq$ 45yrs old) and 25 elderly subjects (aged 45yrs old). The elderly subjects are comprised of both healthy controls (HC) and those with neurological disorders such as mild cognitive impairment (MCI), Frontotemporal Dementia (FTD), and Alzheimer's Disease (AD).

TABLE I
Subject Demographic Data

Diagnosis	Age	Subjects (f/m)	Total
AD	69.9	4 / 4	8
FTD	73.5	0 / 2	2
HC	47.4	11 / 5	16
MCI	72.7	5 / 4	9

The Centiloid Project's FBB calibration dataset [10] includes the following 5 items: (1) a text description of all files, (2) a demographic spreadsheet of all subjects, (3) a spreadsheet containing the SUVr and Centiloid scores of all subjects for different reference regions, (4) a statistical analysis of the SUVr and Centiloid scores (mean, standard deviation, and covariance) for each age group, and (5) the raw DICOM T1-sequenced MRI and FBB PET images for all subjects. GAAIN also provides a $.docx$ file outlining their PiB radiotracer.

B. Software & Tools

SUVr-LW is a python 3.7-based [11] pipeline which uses MRI and PET DICOM files for processing and analysis resulting in the SUVr and centiloid scores of a subject. Figure 1 delineates the SUVr-LW overall flow as follows:

1) Preprocessing: The T1 MRI and FBB PET images provided are in the raw DICOM file format that need to be converted to the more compact NIftI file format. This conversion is done via the popular dcm2niix toolbox [12].

2) MRI Processing: FreeSurfer version 6.0 (FS6) [3] is selected for its active support community and open-source availability allowing for application within the python-based SUVr-LW pipeline. The NIftI formatted T1 images are then routed to FS6 to be processed using the $recon-all$ command which will segment the T1 MRIs according to a stored atlas [13]. This will output the FS6 estimated volumetric information for different regions of the brain.

3) PET Processing: The NIftI PET scans are matched with their T1 NIftI counterparts and the pair of scans are routed to the FSL toolbox [14] for co-registration with the MRI T1 image. Co-registration is achieved using the $flirt$ command with the default settings, e.g. 12 degrees of freedom. The segmented MRIs from Step 2 and the co-registered PET images are used to extract the average intensity of individual ROIs as per Formula 1:

$$C_{roi} = \frac{\sum_{i=1}^{N_{ROI}} K_i}{N_{ROI}} \tag{1}$$

Where C_{roi} is the average intensity of an ROI, K_i represents a voxel intensity, and N_{ROI} is the current ROI calculated. The algorithm parses through all voxels in the PET scan using the FS6 look-up table identifies the most relevant ROI using the x, y, z coordinate of the current voxel. The sum of all intensities for each ROI is stored and divided by the voxel volume of that region yielding the average PET voxel intensity of the region.

4) SUVr Calculation: The SUVr calculation process uses the PET image intensity which is then normalized by Formula 2:

$$SUV_{roi} = \frac{C_{roi}}{B_{inj}} \tag{2}$$
$$where\ B_{inj} = \frac{ID}{BW}$$

Where ID is the injected radio tracer dose and BW the subject's body weight [6]. The SUV quantifies the amount of radiotracer absorbed by the relevant region of the brain. However, since the SUVr, as seen in Formula 3, is needed to compare these values across patient cohorts, an SUV must be normalized to the Whole-Cerebellum (WC) [15].

$$SUVr_{roi} = \frac{SUV_{roi}}{SUV_{ref}} \tag{3}$$

There are many research applications where the purpose of a neuroimaging pipeline is to quantify the incoming neuroimaging scans via volumetric data, SUVr, and centiloid scores, in which can be calculated without the use of the clinical data [16] [17] [18]. Conventionally a subject's B_{inj} is utilized. However, using a mathematical derivation 4 of SUVr formula, the B_{inj} is not necessary to the SUVr or Centiloid score calculations. Instead, SUVr calculations would be reliant on the PET intensity K_{int} and the reference region used to normalize it.

$$SUVr_{roi} = \frac{SUV_{roi}}{SUV_{ref}} = \frac{\frac{C_{roi}}{B_{inj}}}{\frac{C_{ref}}{B_{inj}}} = \frac{C_{roi}}{c_{ref}} \tag{4}$$

5) Centiloid Score Formula: To compare the FBB uptake value to scans across different radiotracers, the global SUVr can be scaled via specific conversion formulae to yield a Centiloid Score [9]. The FBB tracer is scaled via Formula 5 [19].

$$CL_{FBB} = 153.4 \times SUVr_{FBB} - 154.9 \tag{5}$$

6) Analysis: The statistical moments (i.e. mean, median, standard deviation, covariance, and variance) and percent error of the data sets are calculated. WC-normalized SUVrs from GAAIN and SUVr-LW in the study are plotted against each other and the linear regression is calculated for the whole data and across the different age groups. GAAIN's calibration process recommends investigating the correlation among the young control and elderly subject groups. An additional linear regression analysis is also generated considering that the age groups are not further discriminated by diagnostic criteria, such as whether they are healthy controls (HC) or non-healthy controls (NC).

III. Results

A. Individual SUVr/Centiloid Score Comparison between Age Groups

The WC-normalized SUVr scores calculated by SUVr-LW and provided by GAAIN are compared in a scatter plot to produce Figure 2. A linear regression is plotted for each age group. Overall, the data's linear regression had a slope of 0.97. While the elderly subject data is consistent across both methodologies with a linear regression slope of 0.95, the young control group has a slope of 0.54. This graph is replicated with the WC-normalizedd Centiloid Scores as seen in Figure 3. The linear regression for all groups produced a slope of 0.97, the elderly a slope of 0.95, and the young controls a slope 0.54.

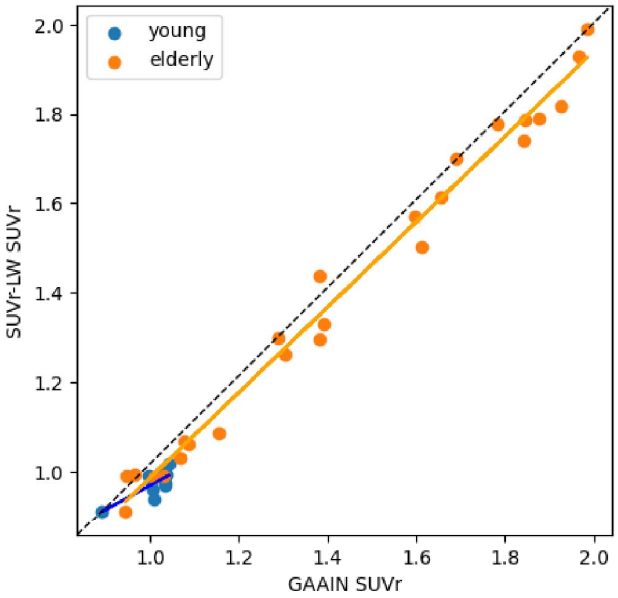

Fig. 2. WC SUVr scatter plot with 1:1 and linear regression across Young and Elderly age groups.

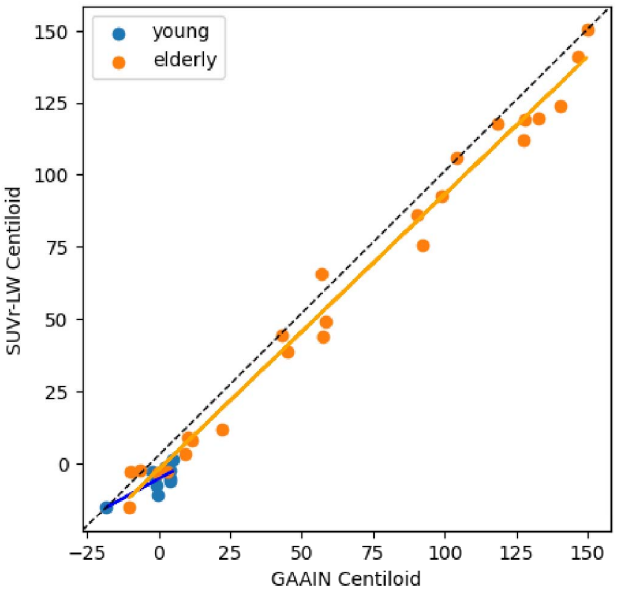

Fig. 3. WC Centiloid scatter plot with 1:1 and linear regression across Young and Elderly age groups.

B. Individual SUVr/Centiloid Score Comparison between Diagnostic Groups

The results are grouped by diagnostic criteria (HC / NC) and a linear regression for each group is plotted as seen in Figure 4. The HC group has a linear regression slope of 0.87 and the NC group a slope of 0.96.

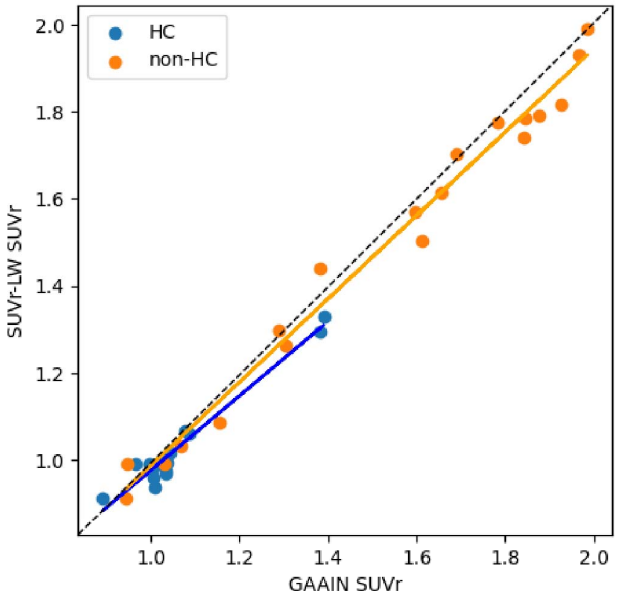

Fig. 4. WC SUVr scatter plot with 1:1 and linear regression across diagnostic groups health control (HC) and non-control (non-HC).

C. Histogram Analysis

The SUVr of both pipelines are plotted on overlaying histograms to better visualize the overall shape and the differences between both methods as seen in Figure 5, and the kernel density estimation lines for each dataset were plotted in Figure 6.

TABLE II
SUVR STATISTICAL ANALYSIS

Age Group	Method	Mean	Median	StD	Cov	Var
Elderly	SUVr-LW	1.4	1.33	0.35	0.25	0.12
	GAAIN	1.43	1.38	0.36	0.25	0.13
Young	SUVr-LW	0.97	0.98	0.03	0.03	0
	GAAIN	1.01	1.02	0.04	0.04	0

IV. CONCLUSION

Overall, the results suggest that there is a high correlation between the GAAIN processed-results and the SUVr-LW pipeline. In Figure 2, the scatter plot values of the individual subject SUVrs initially appear to have significant variance. However, upon further analysis, SUVR-LW's overall results

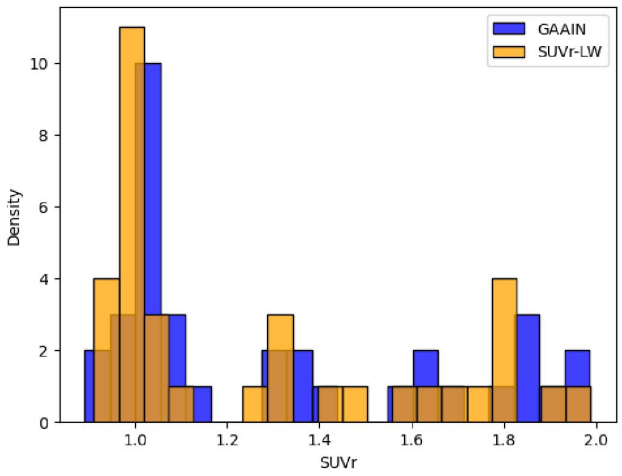

Fig. 5. Histogram of SUVr for GAAIN and SUVR-LW.

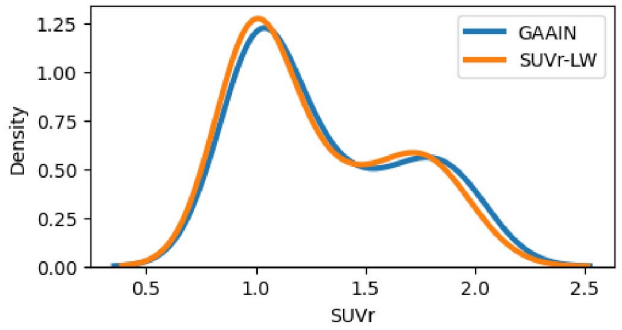

Fig. 6. Kernel Mean Density plot of SUVr for GAAIN and SUVR-LW.

remain consistent when compared with the GAAIN FBB PET calibration dataset. The linear regression plots seen in Figure 2 and Figure 3 illsutrate the close correlation among the elderly data group.

The strongest correlation of SUVrs between SUVr-LW and GAAIN occurs within the elderly age group with a linear regression slope of 0.97. In the multi-diagnostic linear regression plot generated in Figure 4, SUVr-LW exhibits a high correlation with the GAAIN calibration dataset across both diagnostic categories where the health controls' linear regression slope is 0.87 and 0.96 for the non-healthy controls. The histogram from Figure 5 of the SUVr data indicate a strong correlation by the general shape of both datasets is relatively similar with a slight deviation explained by the different softwares used. This visual analysis is confirmed via statistical analysis where the mean percent difference for elderly age group between the GAAIN and SUVr-LW 2.43% and 3.57% for the young group.

A. Limitations

From Figure 2, the young age group's linear regression slope is 0.54 which implies poor correlation for this group.

The inconsistency between the young control groups could potentially be caused by the small sample size of 10 young controls.

Additionally, it should be noted that both pipelines use different software and methodologies with SUVr-LW using FreeSurfer while the GAAIN pipeline employs the SPM toolbox [4] for the MRI processing. These two softwares have been shown to skew the MRI volumetric data in different ways, such as enlarging white matter regions with respect to the other [20]. As for the PET coregistration, SUVr-LW uses FSL and GAAIN makes use of SPM. These differences can cause discrepancies inherent to the tool being used and must be considered when evaluating results from different pipelines.

B. Future Work

In future studies, a larger dataset should be used from a prominent AD neurogimaging database such as the Alzheimer's Disease Neuroimaging Initiative (ADNI) [21]. Additionally, SUVr-LW should be evaluated using other radiotracers besides FBB, such as PiB, FDG, and AV45, to ensure the consistency of the pipeline. Lastly, different reference regions should be used for the SUVr to test the consistency of SUVr-LW methodologies. Furthermore, the discrepancy between the slope of the elderly population and young control population should be further investigated to ascertain the source of the inconsistent SUVr values.

This study aims to serve as the beginning of investigative studies on the stability and robustness of different SUVr variables, such as determining the optimal K_{int} PET value and reference region used in normalization. This should in-turn provide the most accurate and relevant information for AD neuroimaging research.

ACKNOWLEDGMENTS

This research is supported by the National Science Foundation under grants: CNS-1920182, CNS-2018611, and CNS-1551221, and with the National Institutes of Health through the P30AG066506 with the 1Florida Alzheimer's Disease Research Center (ADRC).

REFERENCES

[1] C. R. Jack, M. S. Albert, D. S. Knopman, G. M. McKhann, R. A. Sperling, M. C. Carrillo, B. Thies, and C. H. Phelps, "Introduction to the recommendations from the National Institute on Aging-Alzheimer's Association workgroups on diagnostic guidelines for Alzheimer's disease," *Alzheimers Dement*, vol. 7, no. 3, pp. 257–262, May 2011.

[2] J. Weller and A. Budson, "Current understanding of Alzheimer's disease diagnosis and treatment," *F1000Res*, vol. 7, pp. F1000 Faculty Rev–1161, Jul. 2018.

[3] FreeSurfer. FreeSurfer. [Online]. Available: https://surfer.nmr.mgh.harvard.edu (Accessed 2022-10-17).

[4] SPM - Statistical Parametric Mapping. [Online]. Available: https://www.fil.ion.ucl.ac.uk/spm/ (Accessed 2022-10-18).

[5] C. M. Clark, C. Davatzikos, A. Borthakur, A. Newberg, S. Leight, V. M.-Y. Lee, and J. Q. Trojanowski, "Biomarkers for Early Detection of Alzheimer Pathology," *NSG*, vol. 16, no. 1, pp. 11–18, 2008.

[6] J. W. Keyes, "SUV: Standard uptake or silly useless value?" *J Nucl Med*, vol. 36, no. 10, pp. 1836–1839, Oct. 1995.

[7] S. Bullich, V. L. Villemagne, A. M. Catafau, A. Jovalekic, N. Koglin, C. C. Rowe, and S. D. Santi, "Optimal Reference Region to Measure Longitudinal Amyloid-β Change with 18F-Florbetaben PET," *Journal of Nuclear Medicine*, vol. 58, no. 8, pp. 1300–1306, Aug. 2017.

[8] V. L. Villemagne, M. T. Fodero-Tavoletti, K. E. Pike, R. Cappai, C. L. Masters, and C. C. Rowe, "The ART of Loss: Aβ Imaging in the Evaluation of Alzheimer's Disease and other Dementias," *Mol Neurobiol*, vol. 38, no. 1, pp. 1–15, Aug. 2008.

[9] W. E. Klunk, R. A. Koeppe, J. C. Price, T. L. Benzinger, M. D. Devous, W. J. Jagust, K. A. Johnson, C. A. Mathis, D. Minhas, M. J. Pontecorvo, C. C. Rowe, D. M. Skovronsky, and M. A. Mintun, "The Centiloid Project: Standardizing quantitative amyloid plaque estimation by PET," *Alzheimer's & Dementia*, vol. 11, no. 1, pp. 1–15.e4, Jan. 2015.

[10] The Global Alzheimer's Association Interactive Network. [Online]. Available: https://gaain.org/centiloid-project/ (Accessed 2022-10-15).

[11] Welcome to Python.org. Python.org. [Online]. Available: https://www.python.org/ (Accessed 2022-10-18).

[12] "Rordenlab/dcm2niix," Chris Rorden's Lab. [Online]. Available: https://github.com/rordenlab/dcm2niix (Accessed 2022-10-17).

[13] B. Fischl, D. H. Salat, E. Busa, M. Albert, M. Dieterich, C. Haselgrove, A. van der Kouwe, R. Killiany, D. Kennedy, S. Klaveness, A. Montillo, N. Makris, B. Rosen, and A. M. Dale, "Whole brain segmentation: Automated labeling of neuroanatomical structures in the human brain," *Neuron*, vol. 33, no. 3, pp. 341–355, Jan. 2002.

[14] M. Jenkinson, P. Bannister, M. Brady, and S. Smith, "Improved optimization for the robust and accurate linear registration and motion correction of brain images," *Neuroimage*, vol. 17, no. 2, pp. 825–841, Oct. 2002.

[15] S. K. Royse, D. S. Minhas, B. J. Lopresti, A. Murphy, T. Ward, R. A. Koeppe, S. Bullich, S. DeSanti, W. J. Jagust, and S. M. Landau, "Validation of amyloid PET positivity thresholds in centiloids: A multisite PET study approach," *Alzheimers Res Ther*, vol. 13, p. 99, May 2021.

[16] Y. Yan, E. Somer, and V. Grau, "Classification of amyloid PET images using novel features for early diagnosis of Alzheimer's disease and mild cognitive impairment conversion," *Nuclear Medicine Communications*, vol. 40, no. 3, pp. 242–248, Mar. 2019.

[17] F. Reith, M. Koran, G. Davidzon, and G. Zaharchuk, "Application of Deep Learning to Predict Standardized Uptake Value Ratio and Amyloid Status on ^{18} F-Florbetapir PET Using ADNI Data," *AJNR Am J Neuroradiol*, vol. 41, no. 6, pp. 980–986, Jun. 2020.

[18] P. Raniga, P. Bourgeat, J. Fripp, O. Acosta, V. L. Villemagne, C. Rowe, C. L. Masters, G. Jones, G. O'Keefe, O. Salvado, and S. Ourselin, "Automated 11C-PiB Standardized Uptake Value Ratio," *Academic Radiology*, vol. 15, no. 11, pp. 1376–1389, Nov. 2008.

[19] C. C. Rowe, V. Doré, G. Jones, D. Baxendale, R. S. Mulligan, S. Bullich, A. W. Stephens, S. De Santi, C. L. Masters, L. Dinkelborg, and V. L. Villemagne, "18F-Florbetaben PET beta-amyloid binding expressed in Centiloids," *Eur J Nucl Med Mol Imaging*, vol. 44, no. 12, pp. 2053–2059, Nov. 2017.

[20] L. Palumbo, P. Bosco, M. E. Fantacci, E. Ferrari, P. Oliva, G. Spera, and A. Retico, "Evaluation of the intra- and inter-method agreement of brain MRI segmentation software packages: A comparison between SPM12 and FreeSurfer v6.0," *Physica Medica*, vol. 64, pp. 261–272, Aug. 2019.

[21] S. G. Mueller, M. W. Weiner, L. J. Thal, R. C. Petersen, C. R. Jack, W. Jagust, J. Q. Trojanowski, A. W. Toga, and L. Beckett, "Ways toward an early diagnosis in Alzheimer's disease: The Alzheimer's Disease Neuroimaging Initiative (ADNI)," *Alzheimer's & Dementia*, vol. 1, no. 1, pp. 55–66, Jul. 2005.